Beam polarimetry in the NICA collider using a proton cluster target

N. Piskunov
Joint Institute for Nuclear Research, 141980 Dubna, Russia

In collaboration with: R. Shindin, D. Kirillov, A. Druzhinin, V. Fimushkin, A. Galoyan, O. Gavrishchuk, V. Uzhinsky, D. Toropkov

4.4.1. NICA luminosity.

The NICA luminosity in the polarized proton mode is estimated for the proton kinetic energy region from 1 to 12.7 GeV [11], Fig. 4.7.

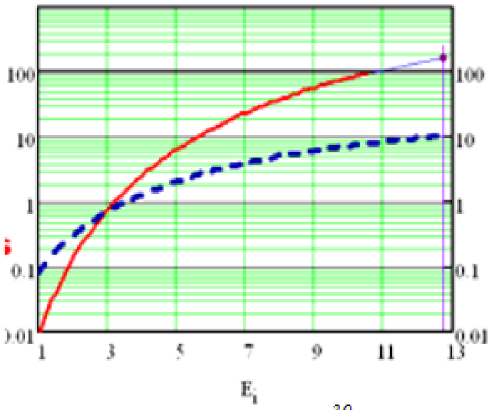

Fig. 4.7: *NICA pp luminosity in units 10^{30} (left scale, solid line) and the number of particles per bunch in units 10^{11} cm^{-2} s^{-1} (right scale, dotted line) vs. the proton kinetic energy.*

The luminosity and total number of the stored particles has been calculated taking into account the beam space charge limits and other parameters listed below.

Parameters of NICA: circumference - 503 m,
number of intersection points (IP) - 2,
beta function β_{min} in the IP - 0.35 m,
number of protons per bunch - $\sim 1 \cdot 10^{12}$,
number of bunches - 22,
RMS bunch length - 0.5 m,
incoherent tune shift, $\Delta_{Lasslett}$ - 0.027,
beam-beam parameter, ξ - 0.067,
beam emittance ε_{nrm}, π mm mrad - 0.15 (normalized at 12.5 GeV).

The number of particles reaches a value about $2.2 \cdot 10^{13}$ in each ring and the peak luminosity $L_{peack} = 2 \cdot 10^{32}$ $cm^{-2}s^{-1}$ at 12.7 GeV. Assuming the cooling time $T_{cool} = 1500$ s, the luminosity life time $T_{Llf} = 20000$ s with the beam polarization not less than 70% and the machine reliability coefficient $k_r = 0.95$, the average luminosity will be $L_{aver} = L_{peack} \cdot 0.86$ or $1.7 \cdot 10^{32}$ cm^{-2} s^{-1} [12] during the working time of the complex.

So, feasible schemes of manipulations with polarized protons and deuterons are suggested [10, 14]. The final scheme of the polarized proton acceleration up to required energy and beam manipulations at NICA will be approved at the later stages of the NICA project.

NICA collider

22 bunches

2.2 x 10^13 protons in each ring

1 x 10^12 protons per bunch

0.5 m RMS bunch length ~ 3 ns

1.68 μs

$$\text{Lumi} = \frac{N_1 * N_2 * f * n_b}{4 * \pi * \sigma_x * \sigma_y}$$

Nuclotron ring

upto 5 bunches or continuous

upto 5 x 10^10 protons in ring

0,835 μs

bunch length ~ 80 ns

Lumi = $N/s * \rho_t * l$

Reactions that can used in polarimetry

1-13 GeV/c

	Type of reaction	Cross-section/ Total cross-section	Analyzing power
1	pp scattering Elastic pp Quasi-elastic (CH2) CNI	 4 – 2 mb/~40 mb ~ 6-3 mb/~400 mb ~ 2 mb /~40 mb	 (20 -7) % <20 % 4.5 %
2	Charge-exchange reactions p-> n pp-> n+X	 < 1 mb /~45 mb 0,07 mb /~45 mb	 up to 30% ~ 7%
3	Inclusive pion production	~ 30 μb /~40 mb	up to 30%
4	Elastic proton-electron scattering	~ /~2000 b at 10 GeV	

$$A_y \bullet P_y = \frac{N_L - N_R}{N_L + N_R}$$

Principle of Polarimetry

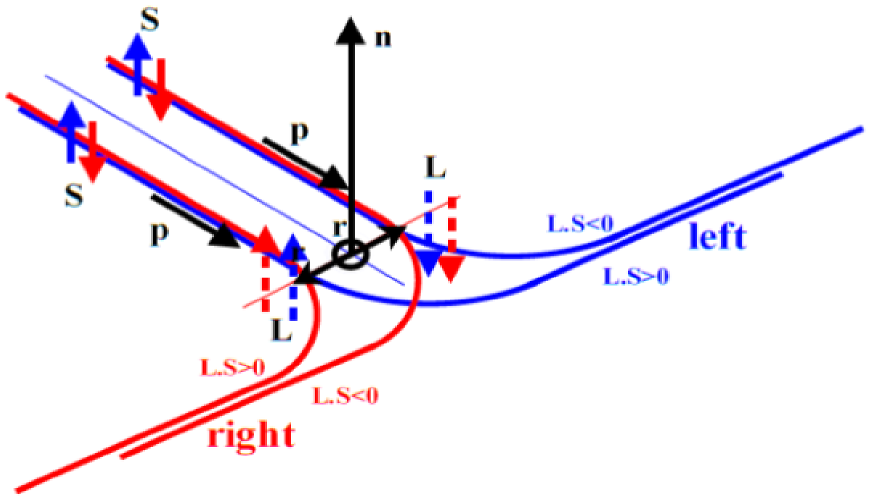

Due to **L.S** coupling in NN interaction, incident particle with spin up or spin down relative to scattering plane scatters preferentially left, respectively right.

Azimuthal distribution:

$$I(\vartheta)=I_0[1+A_y(\vartheta)\vec{P}^{\mathrm{fpp}}.\vec{n}]$$

Following Basel convention (1960), spin-$\frac{1}{2}$ particles with spin up scatter preferentially to the left if analyzing power, Ay, is positive

Spin 1/2
$$\frac{d\sigma}{d\Omega}(\Theta,\phi) = \left(\frac{d\sigma}{d\Omega}\right)_0(\Theta)\left[1+\frac{1}{2}p_y A_y(\Theta)\right]$$

Spin 1
$$\frac{d\sigma}{d\Omega} = \left(\frac{d\sigma}{d\Omega}\right)_0\left[1+\frac{3}{2}p_y A_y+\frac{1}{2}p_{zz}A_{zz}+\frac{2}{3}p_{xz}A_{xz}+\frac{1}{6}(p_{xx}-p_{yy})(A_{xx}-A_{yy})\right]$$

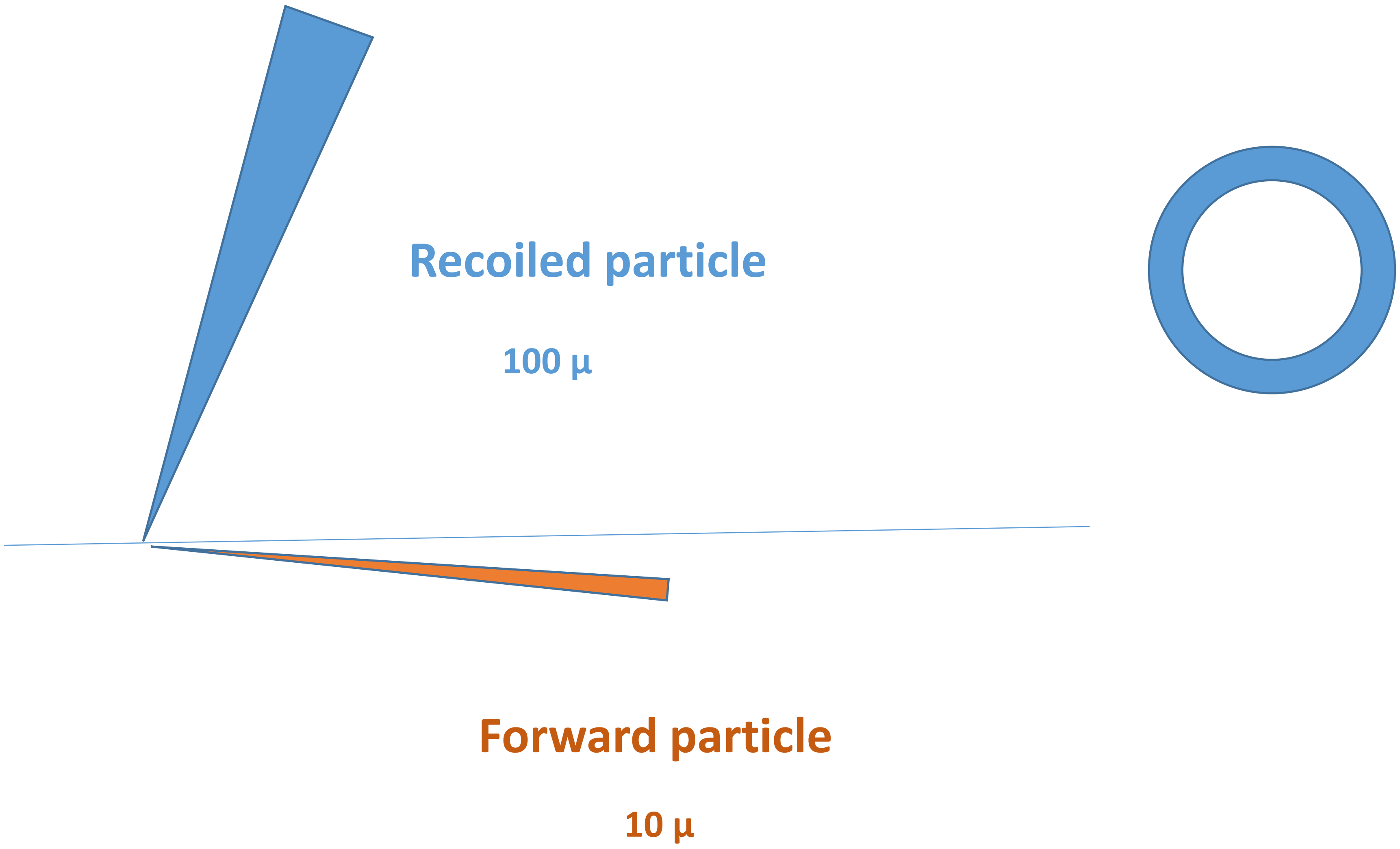

Recoiled particle
100 μ
Forward particle
10 μ

1.3.4 Hardware Trigger

The first level trigger relies solely on the outer layer. The *coplanar trigger* requires coincident signals in two opposite scintillating bars (**B**). It takes advantage of the coplanarity of two protons in the final state, as expressed by the following relation between their azimuthal angles ϕ_{p1} and ϕ_{p2}:

$$|\phi_{p1} - \phi_{p2}| = \pi \qquad (1.1)$$

In addition, the kinematic Relation (1.2) between the laboratory angles $\theta_{p1,lab}$ and $\theta_{p2,lab}$ is used for the so called *kinematic trigger*, which relies on signals from the scintillator semi-rings (**R**) and the semi-rings made from scintillating fibers (**F**).

$$\tan\theta_{p1,lab} \cdot \tan\theta_{p2,lab} = 2m_p c^2 / \left(T_p + 2m_p c^2\right) \qquad (1.2)$$

with: m_p: proton mass
T_p: kinetic beam energy

The kinematic Relation (1.2) obviously varies with the kinetic beam energy. To achieve sufficient background suppression, the kinematic trigger is adapted by re-programming it at distinct beam energies during each acceleration cycle.

Example 4.5 The classical method for measuring the polarization of a particle such a proton or neutron is to scatter it from a suitable *analyzing* target and to measur th asymmetry in the scattered particle distribution. One can, for example, count the num ber of particles scattered to the left of the beam at certain angle and to the right of th beam at the same corresponding angle. If R is the number scattered to the right a d the number to the left, the asymmetry is then given by

$$\varepsilon = \frac{R-L}{R+L}.$$

Calculate the error on ε as a function of the counts R and L.

This is a straight forward application of (4.64). Taking ther derivatives of ε, we find

$$\frac{\partial\varepsilon}{\partial R} = \frac{1}{R+L} + \frac{R-L}{(R+L)^2} = \frac{2L}{N_{tot}^2}$$

$$\frac{\partial\varepsilon}{\partial L} = \frac{1}{R+L} + \frac{R-L}{(R+L)^2} = \frac{-2R}{N_{tot}^2},$$

where the total number of counts $N_{tot} = R+L$. The error is thus

$$\sigma^2(\varepsilon) = \frac{4L^2}{N_{tot}^4}\sigma_R^2 + \frac{4R^2}{N_{tot}^4}\sigma_L^2.$$

The covariance is obviously 0 here since the measurements are independent. The e o on R and L are now given by the Poisson distribution, so that $\sigma_R^2 = R$ and $\sigma_L^2 = L$. u stituting into the above, then yields

$$\sigma^2(\varepsilon) = 4\frac{(L^2R+R^2L)}{N_{tot}^4} = 4\frac{RL}{N_{tot}^3}.$$

If the asymmetry is small such that $R \simeq L \simeq N_{tot}/2$, we have the result that

$$\sigma(\varepsilon) \simeq \sqrt{\frac{1}{N_{tot}}}.$$

FOM (Figure of Merit)

p = 5.3 GeV/c

56 cm

one charge particle

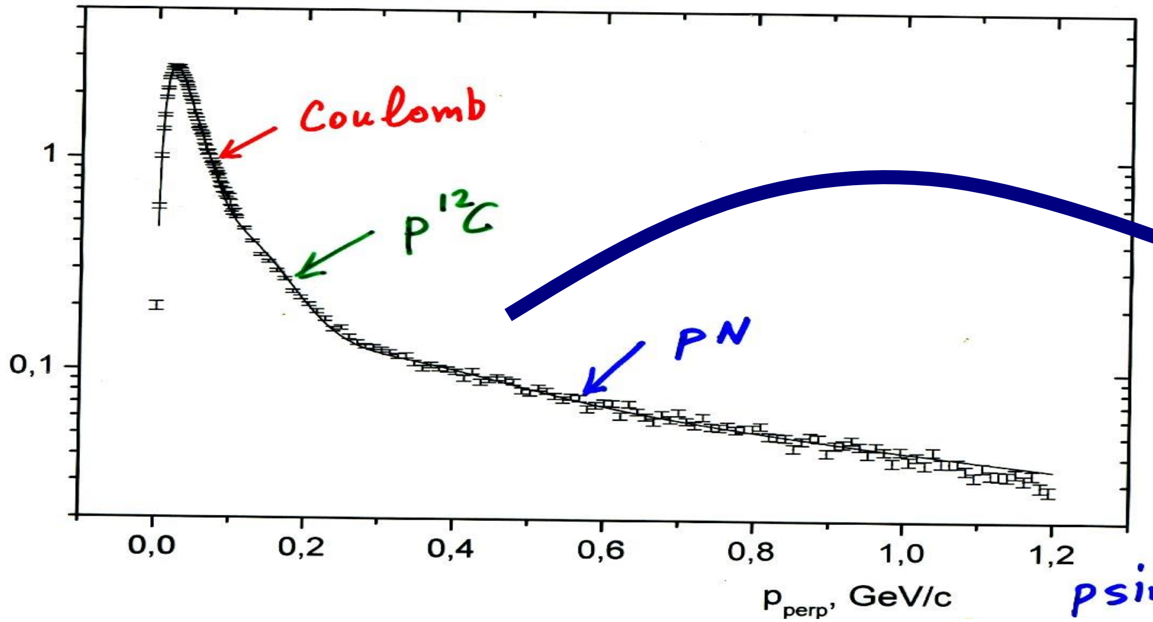

$$F^2 = \int_\theta \varepsilon(\theta) A_y^2(\theta) d\theta$$

$$\Delta P_y = \sqrt{\frac{2}{N_{inc} F^2}}$$

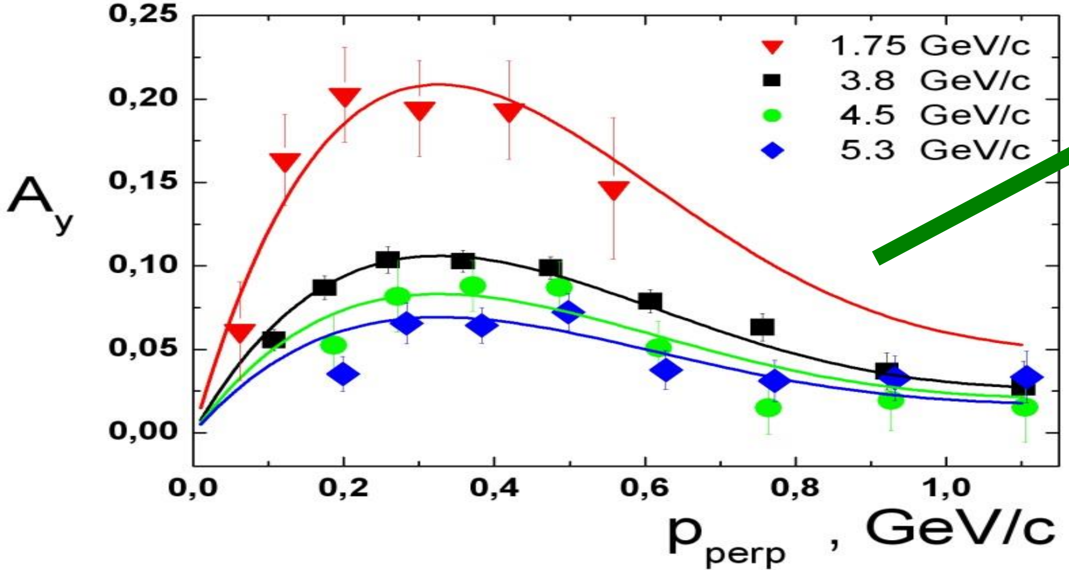

$$\Delta A_y = \frac{1}{P_y} \sqrt{A_y^2 \Delta P_y^2 + \frac{4N^+N^-}{(N^+ + N^-)^3}}$$

$\Delta A_y \sim 0.01$ $N \sim 10^7$

	NICA	
	503 m 1.66 µs 2.2*10^13	
time	turn numbers	
1 s	6.0*10^5	
10 s	6.0*10^6	
1 m	3.6*10^7	
10 m	3.6*10^8	
1 h	2.2*10^9	
10 h	2.2*10^10	

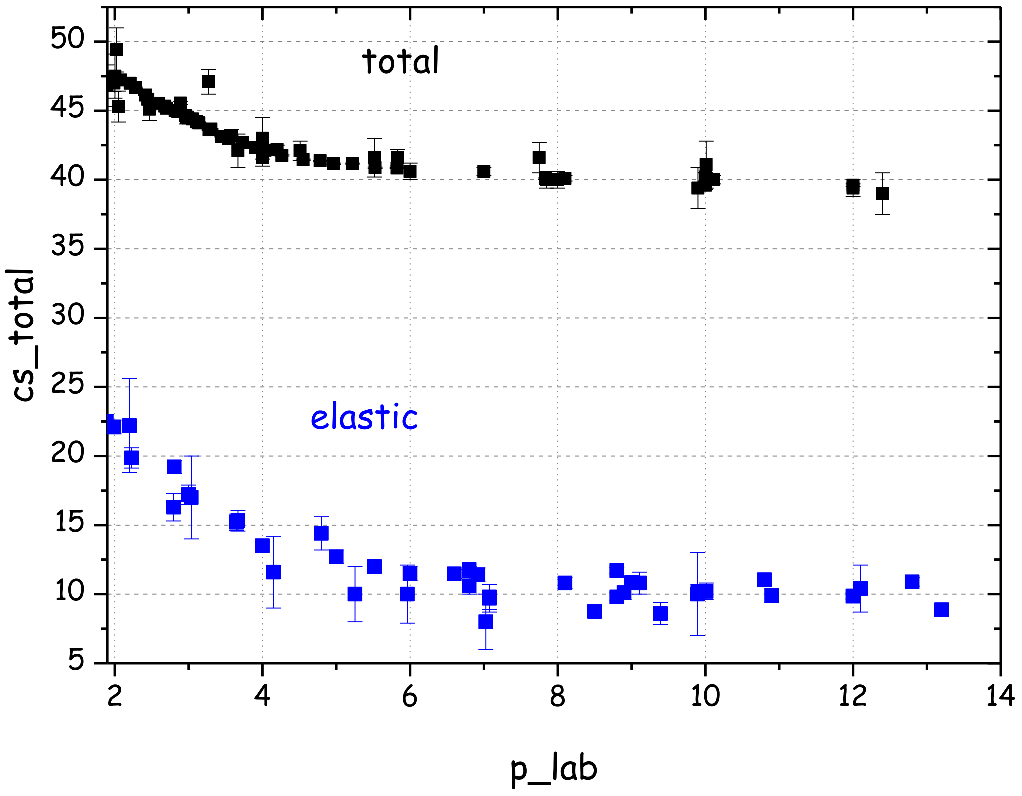

H-jet 1.2*10^12 protons/cm2 σ_{tot} (pp) ~ 40 mb, σ_{el} (pp) ~ 10 mb

H2(D2,CH4)-cluster 10^15 protons/cm2

N_jet = 2.2*10^13 * 1.2*10^12 * 40*10^-27 ~ 1 interaction/turn

N_cluster ~ 10^3

Nuclear Instruments and Methods 211 (1983) 239-261

H.Spinka, 40 years ago

max

Ay

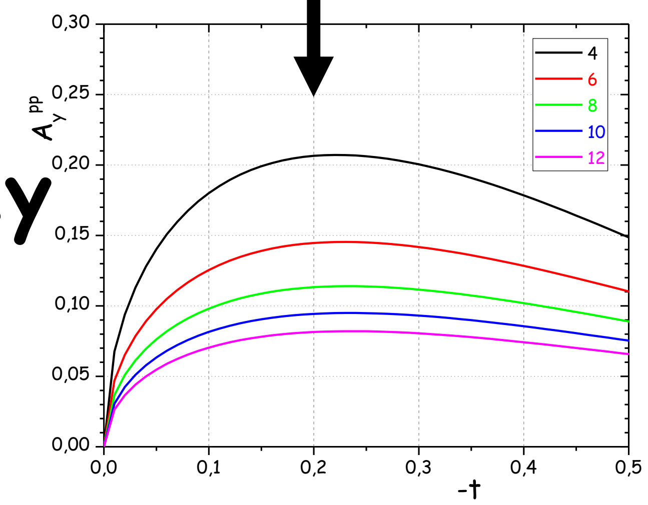

FOM

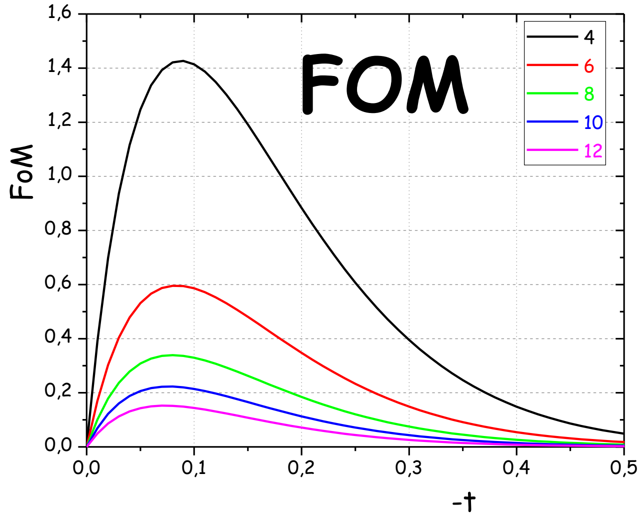

-t, (GeV/c)^2

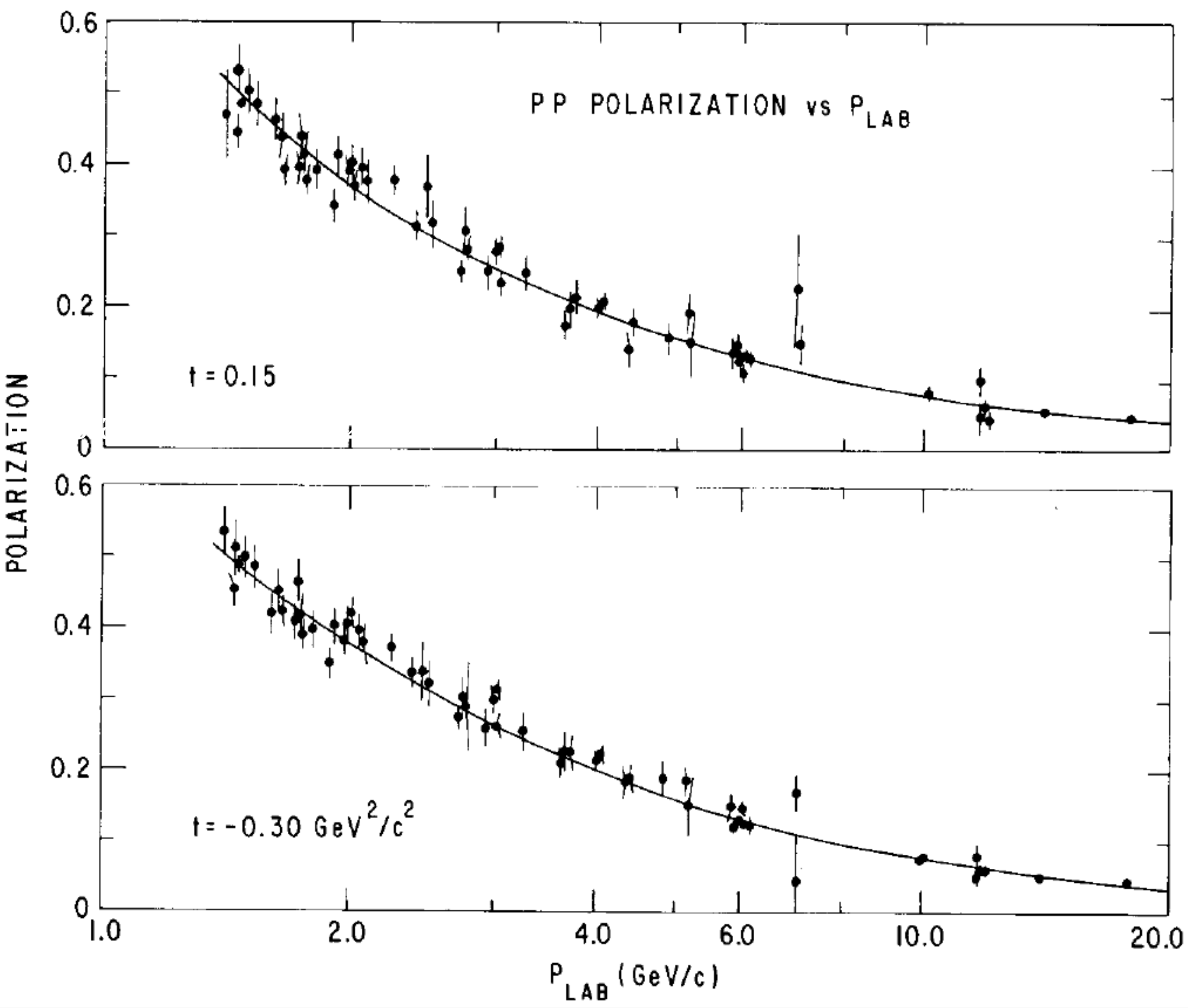

Polarized H-jet target

GeV/c	Δσ, mb 0.1-0.2	An, avr	Δϕ,	Δσ×Δϕ, mb	# turns per event	5%	# turns per 5%	Time
4	3,08	0,195	0,8	2,464	16	1,1 +04	1,8 +05	~ 0,3 s
6	2,56	0,136	0,8	2,048	19	2,2 +04	4,2 +05	~ 0,7 s
8	2,29	0,107	0,8	1,832	22	3,5 +04	7,7 +05	~ 1,3 s
10	2,10	0,088	0,8	1,68	24	5,2 +04	1,2 +06	~ 2,1 s
12	1,84	0,077	0,8	1,472	27	6,9 +04	1,9 +06	~ 3,1 s
	0,0015-0,03							
6, CNI 100, CNI	2.81 1.65	0.030 0.030	0,032 0,032	0,09 0,053	4,4 +02 7,6 +02	4,4 +05 4,4 +05	2,0 +08 3,3 +08	~ 6 m ~ 1.15 h

D. Albers et al.: A Precision Measurement of pp Elastic Scattering Cross Sections at Intermediate Energies

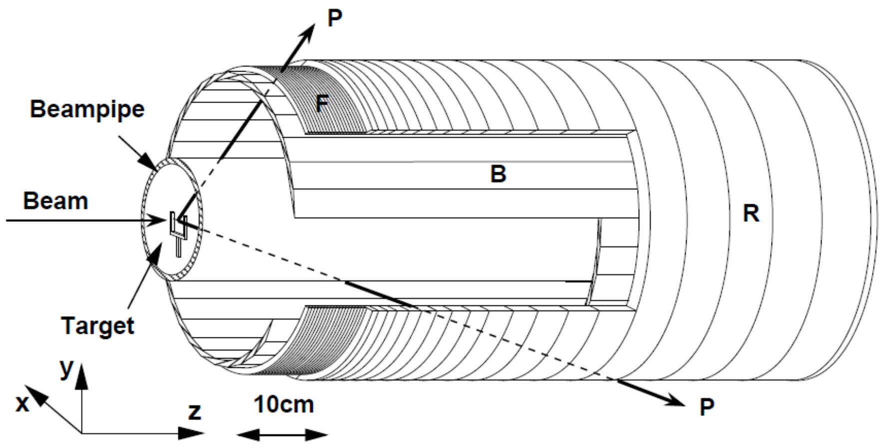

Fig. 1. The EDDA detector (not to scale): target: fiber (CH_2 or C); B: scintillator bars; R: scintillator semi-rings; F: semi-rings made of scintillating fibers.

The structure and granularity of the scintillator hodoscope reflect the signature of pp elastic scattering events, namely (i) coplanarity

$$|\phi_2 - \phi_1| = 180° \quad (1)$$

and (ii) kinematic correlation of scattering and recoil angle, viz

$$\tan\theta_{\mathrm{lab},1} \cdot \tan\theta_{\mathrm{lab},2} = \frac{1}{\gamma^2_{\mathrm{c.m.}}}, \quad (2)$$

where $\gamma_{\mathrm{c.m.}} = \sqrt{1 + T_p/2m_pc^2}$ denotes the Lorentz factor of the pp center–of–mass motion as a function of beam kinetic energy T_p. Both conditions are used to define a fast online trigger.

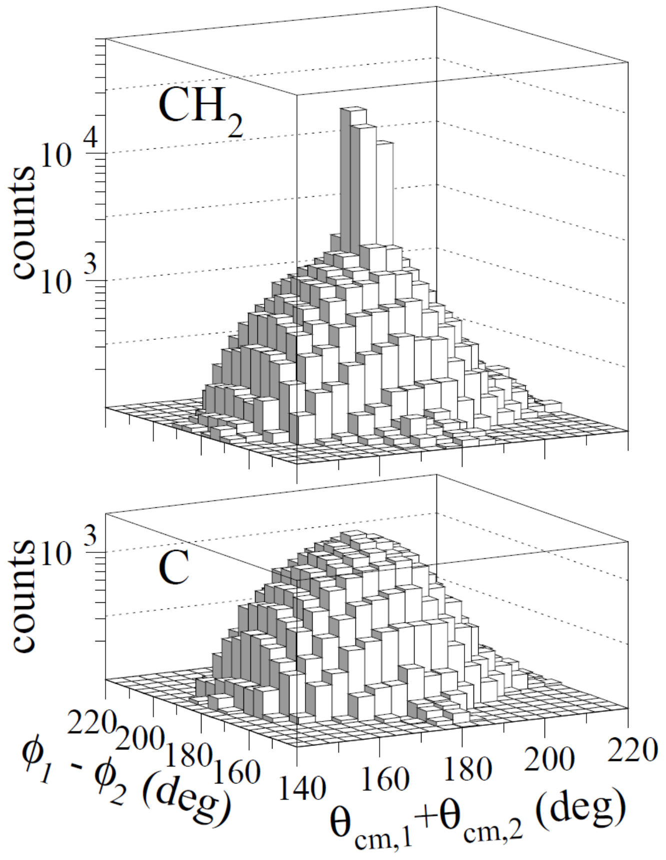

Fig. 8. Distribution of angle integrated events obtained with a CH_2 (top) and carbon (bottom) fiber target at $p = 2.25$ GeV/c. Note the logarithmic scale.

EDDA, COSY, 2004

2 GeV/c

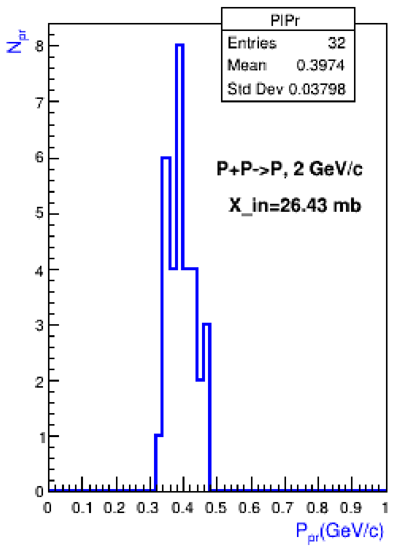

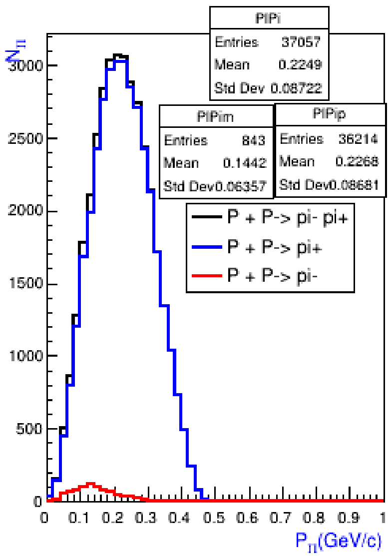

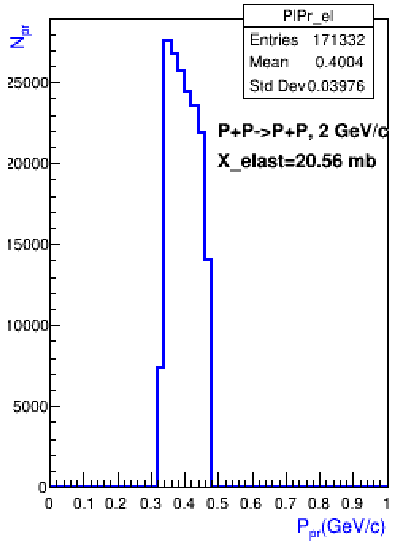

0.22

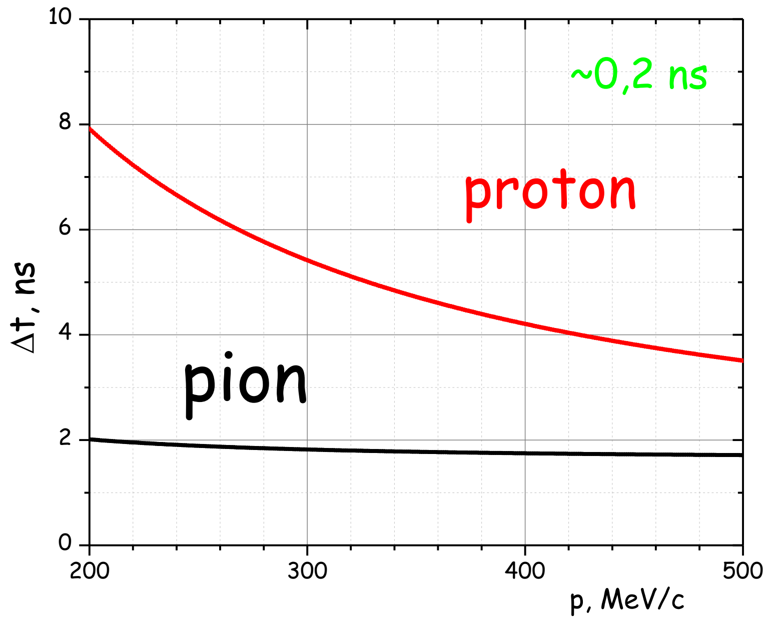

pions

Elastic protons

8 GeV/c

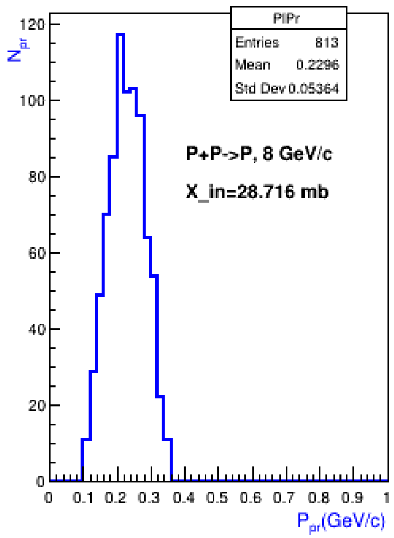

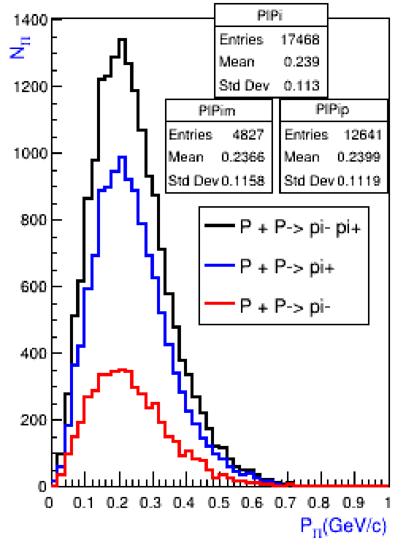

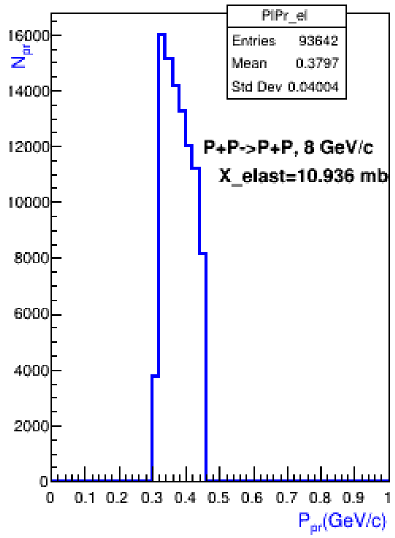

0.18

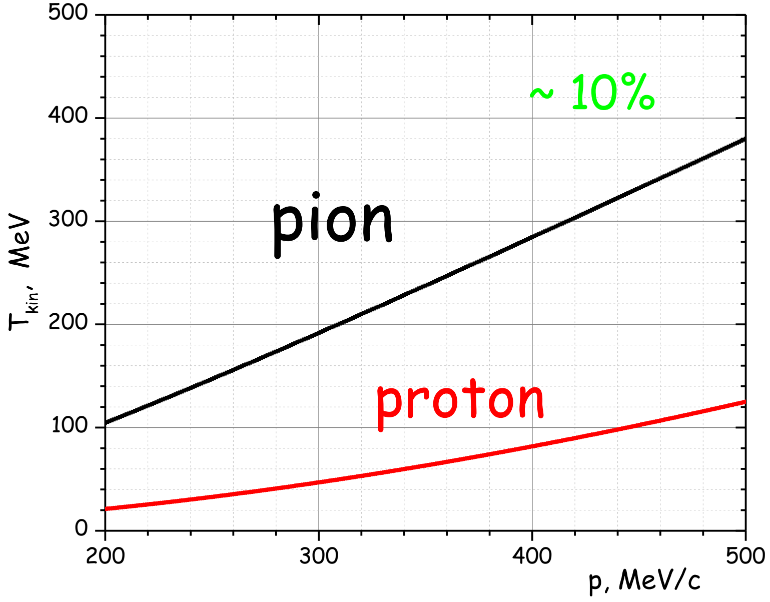

The cluster target

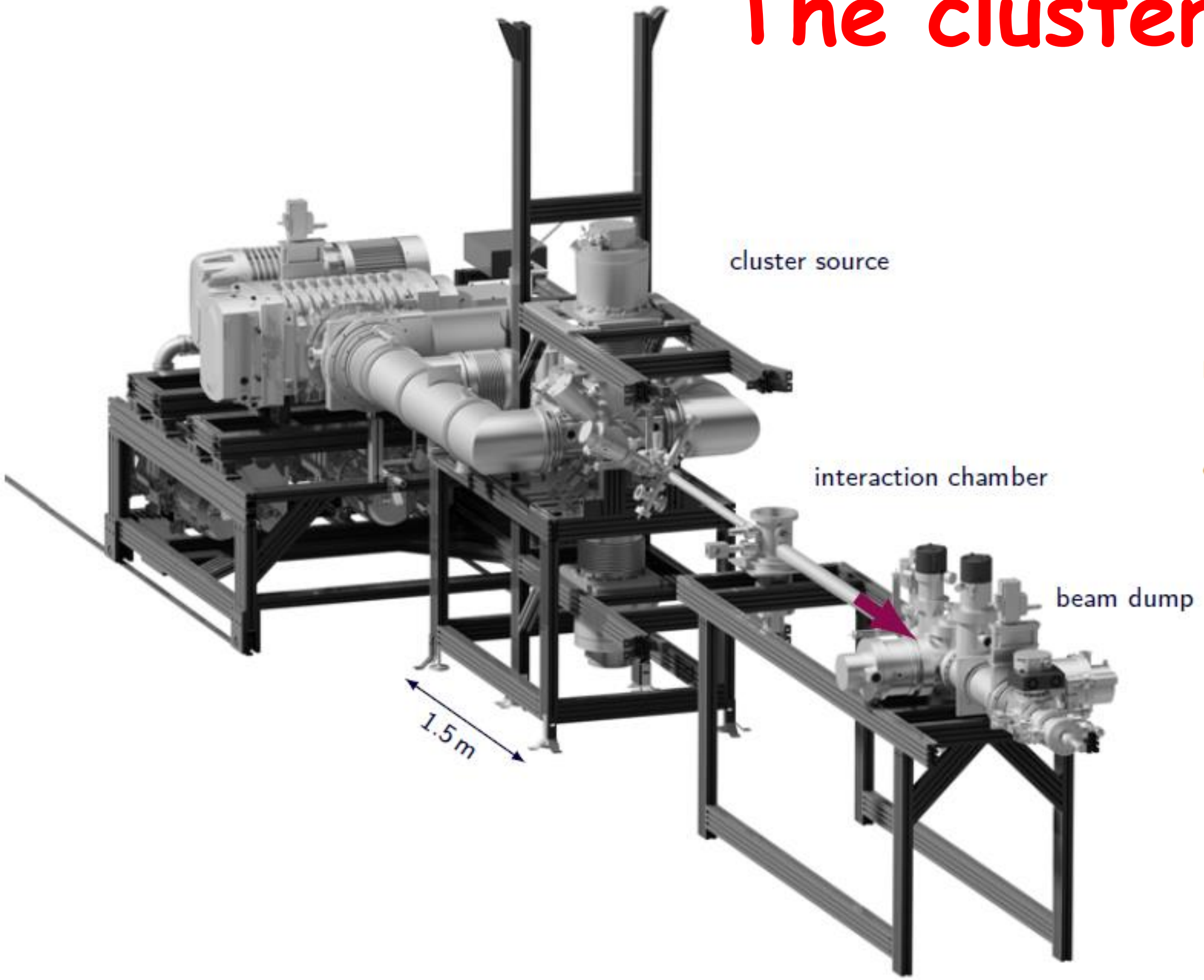

Overview of the cluster-jet target prototype for the PANDA experiment

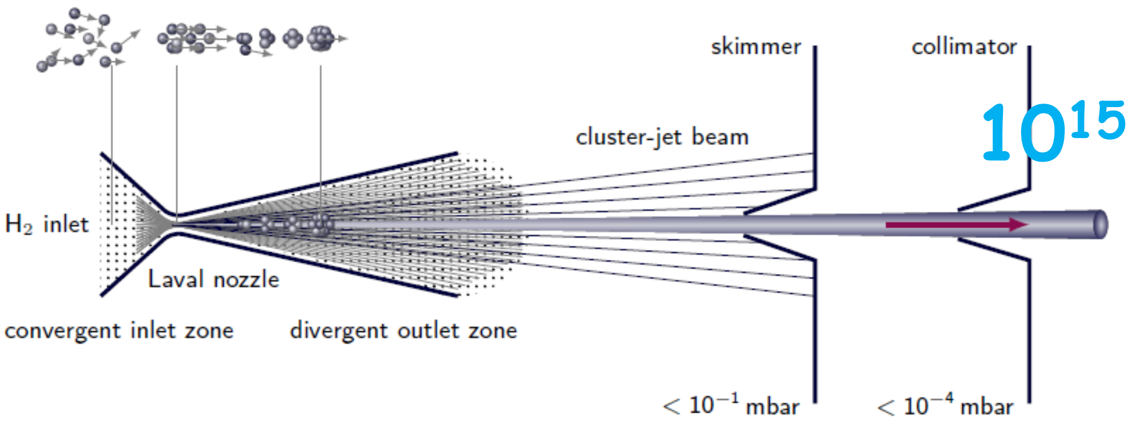

Schematic representation of the cluster production process.

ESPERANZA DIANE KÖHLER

Mass spectroscopy of hydrogen cluster-jets and beam density optimisation studies

The cluster target at the COSY beam

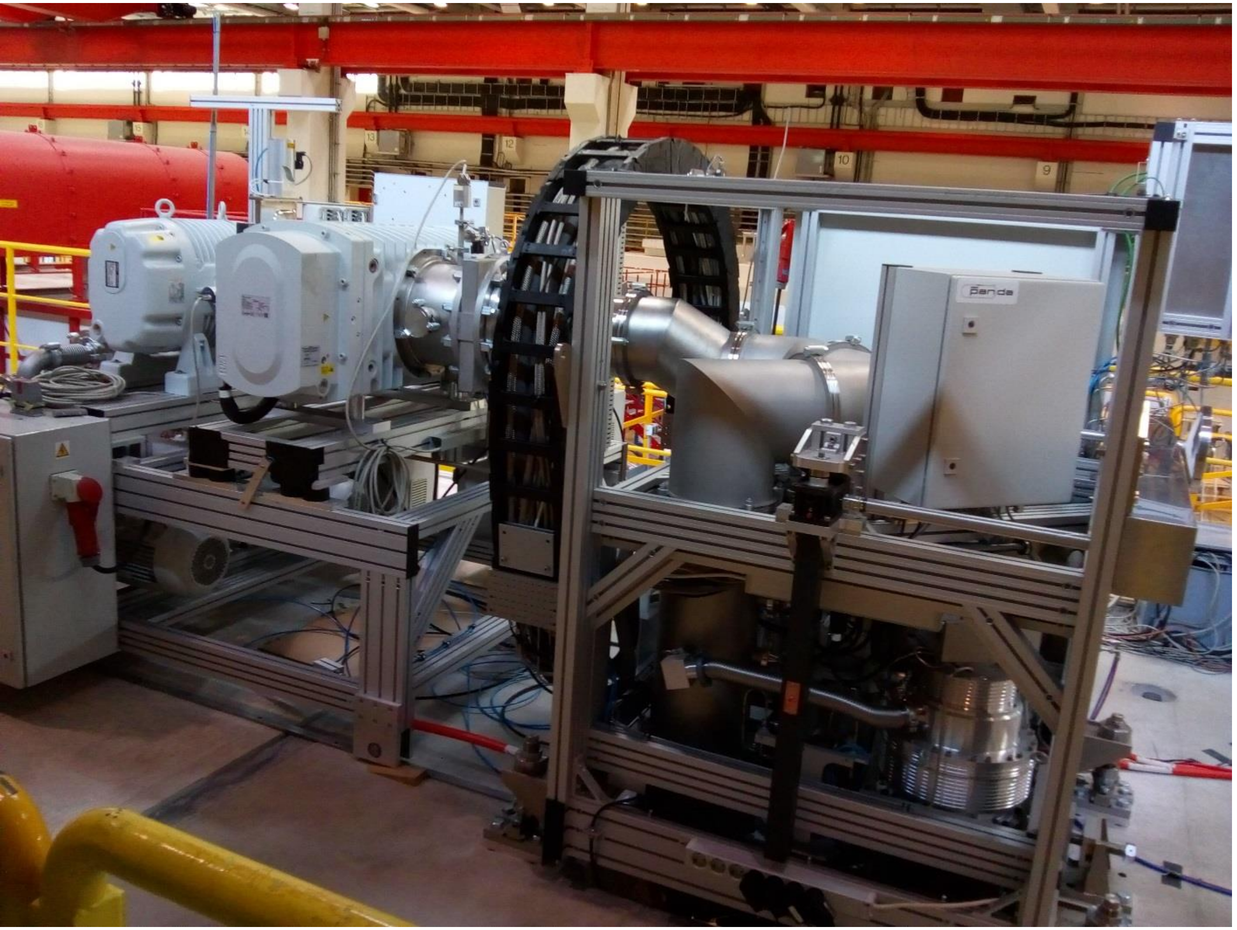

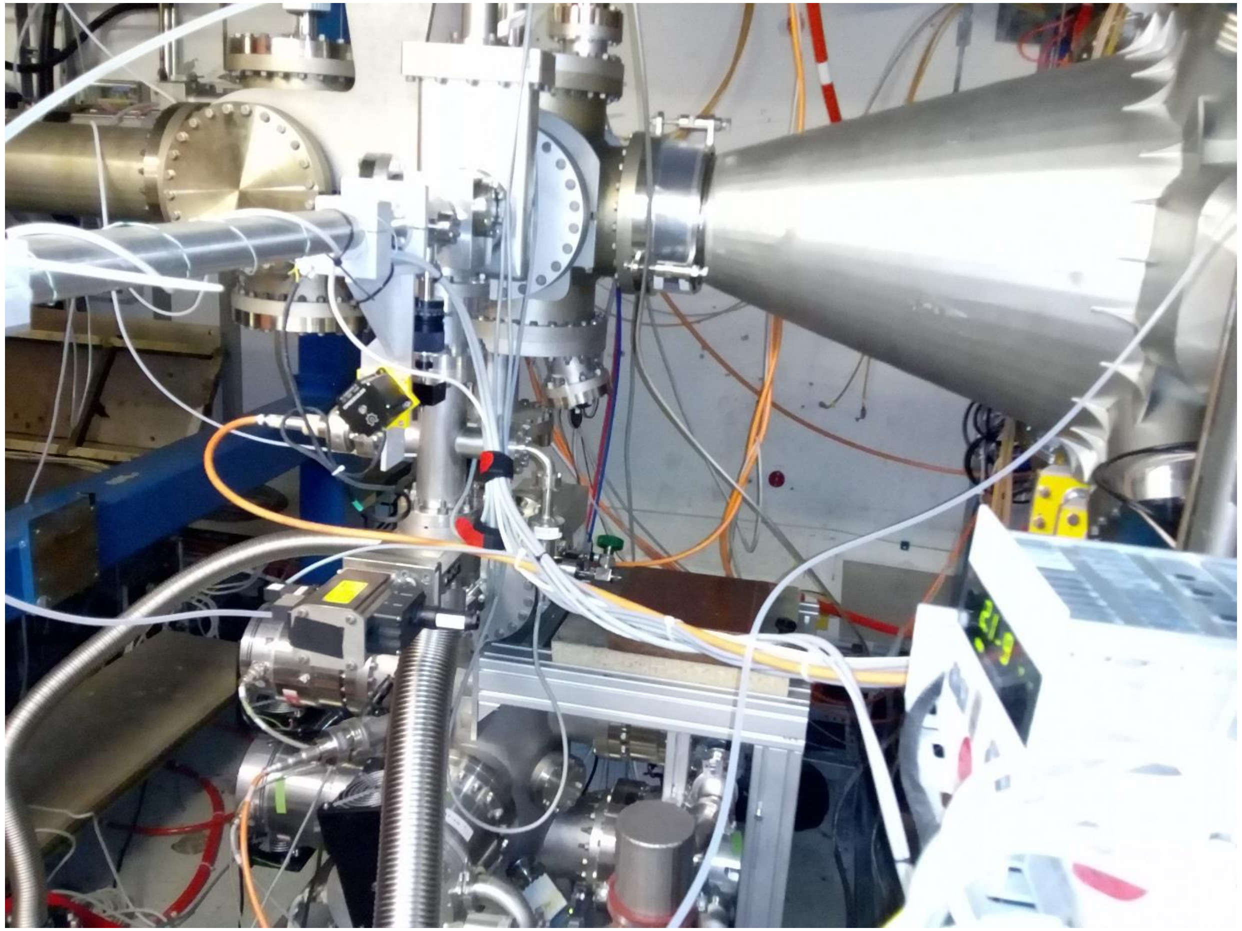

HJet

Left-right asymmetry in elastic scattering: Interference between electromagnetic and hadronic amplitudes in the Coulomb-Nuclear Interference (CNI) region

$$A_N \approx \mathrm{Im}\left(\phi_{SF}^{em}\,\phi_{NF}^{had} + \phi_{SF}^{had\,*}\,\phi_{NF}^{em}\right) / \left|\phi_{NF}^{had}\right|^2$$

Beam and target are both protons

$$A_N(t) = -\frac{\varepsilon_{\text{target}}}{P_{\text{target}}} = \frac{\varepsilon_{beam}}{P_{beam}}$$

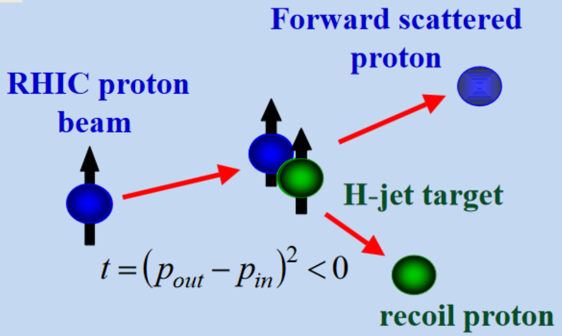

$$\Rightarrow \quad P_{beam} = -P_{\text{target}} \frac{\varepsilon_{beam}}{\varepsilon_{\text{target}}}$$

$$\frac{\Delta P_{\text{beam}}}{P_{\text{beam}}} \approx \frac{\Delta P_{\text{target}}}{P_{\text{target}}} \oplus \frac{\Delta \varepsilon_{\text{target}}}{\varepsilon_{\text{target}}} \oplus \frac{\Delta \varepsilon_{\text{beam}}}{\varepsilon_{\text{beam}}} \quad \text{<5\%}$$

P_{target} is provided by Breit Rabi Polarimeter

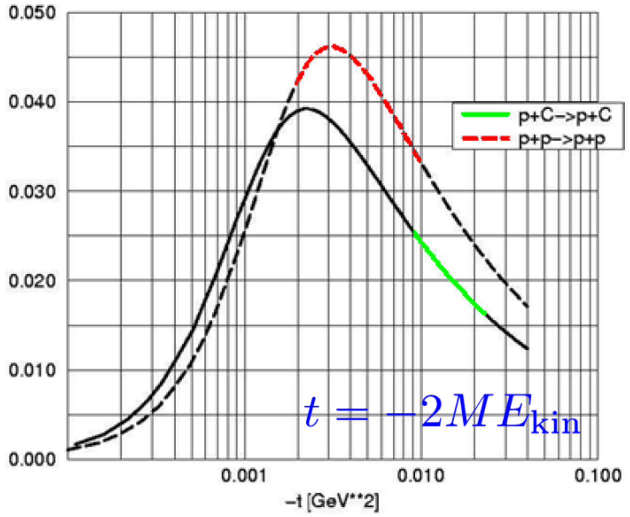

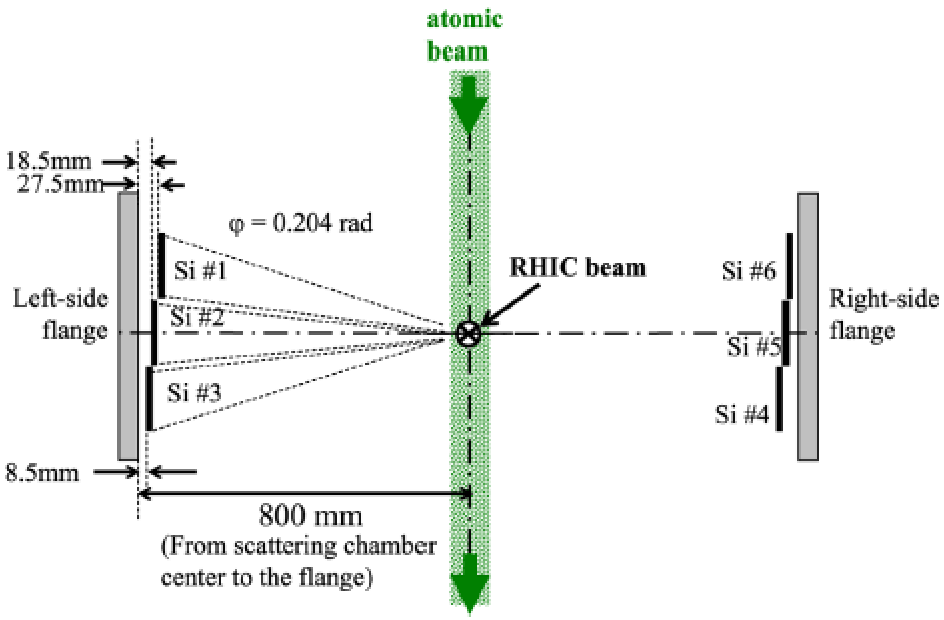

FIG. 2 (color online). Layout of the *pp* elastic scattering setup from the RHIC-beam view. The detectors were mounted on vacuum flanges on the scattering chamber and located to the left and right of the beam. Three pairs of silicon detectors covered an azimuthal angle of 11.7° centered on the horizontal midplane.

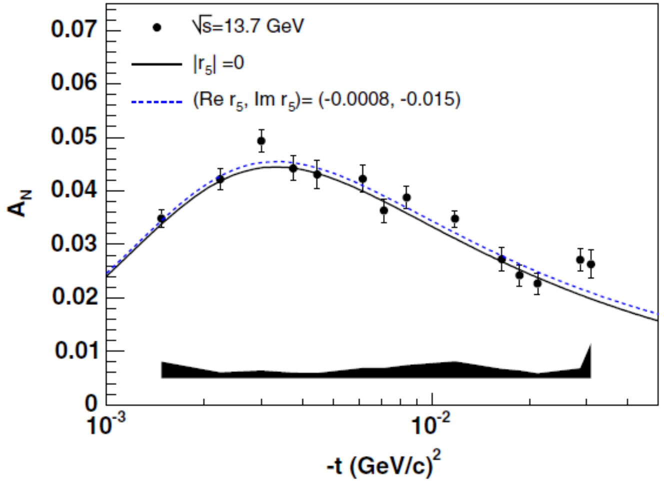

PHYSICAL REVIEW D 79, 094014 (2009)

Recoil protons

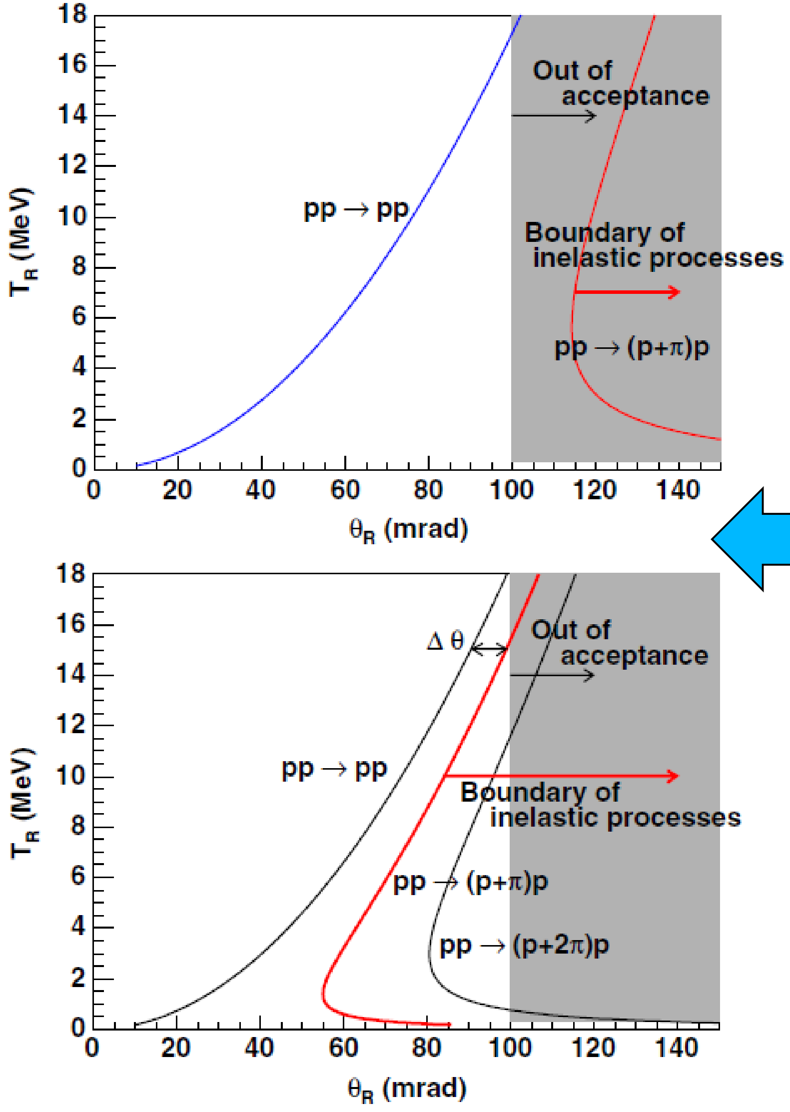

FIG. 12 (color online). Top: Calculation of T_R-θ_R correlation for $pp \to pp$ and inelastic process at $\sqrt{s} = 6.8$ GeV. Detectors cover $10 < \theta_R < 100$ mrad. Bottom: The same for $\sqrt{s} = 13.7$ GeV. The difference between the recoil angle of the elastic process and inelastic processes, $\Delta\theta$, decreases as T_R increases and $\Delta\theta = 8.3$ mrad at $T_R = 15$ MeV.

Elastic pp

CNI

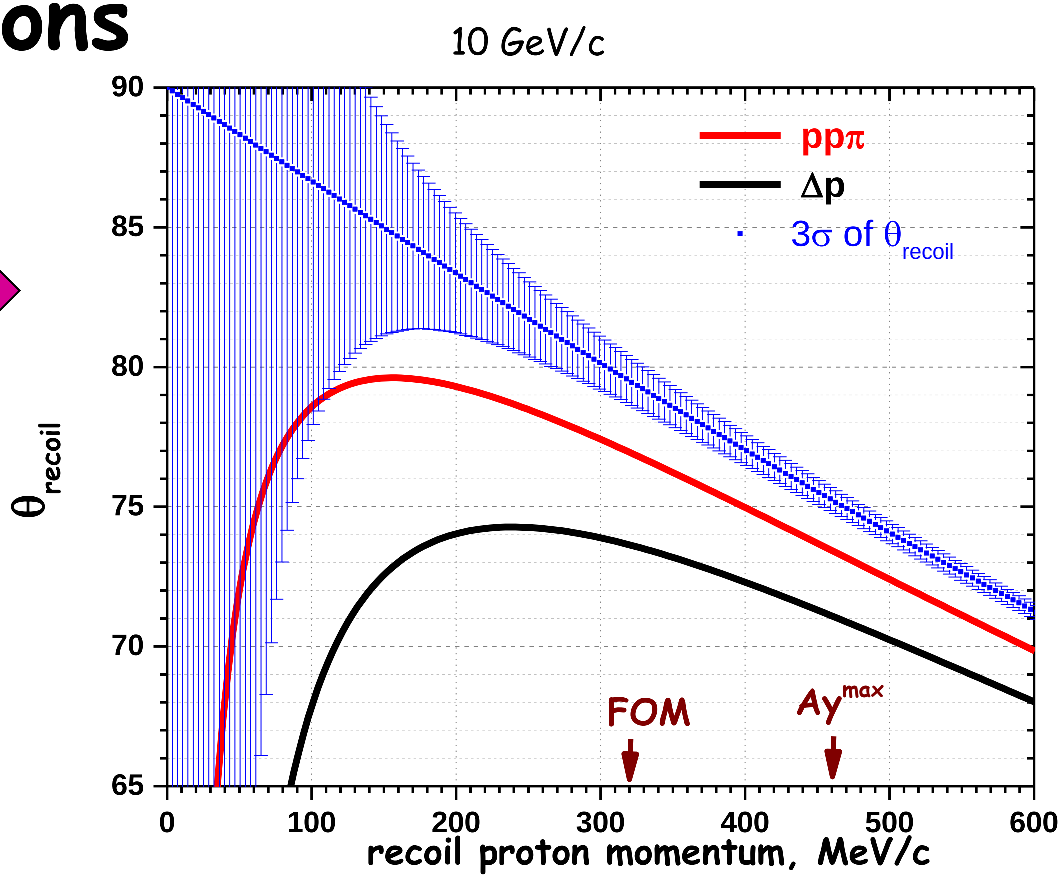

0,3-0,5 GeV/c

CONCLUSION

Elastic pp scattering with detecting scattered and recoil protons is the best reaction for proton polarimetry in momentum interval from 1 to 13 GeV/c

A cluster target (protons or deuterons or Argon) should be installed in NICA ring

Thank you!

Section 2
Work program, budget and time schedule

Main research goal:

Based on the results that have been obtained at WWUM in construction of the cluster jet target the main research goals are formulated as the following:

a) Design, construction and production of the moveable jet target and a preliminary test of the target at WWUM.

b) Test of the moveable cluster target at the beam in JINR.

It is proposed that:

a) After completion of the work program the obtained test data provide all information needed for operation of the moveable cluster jet target: gas molecules H_2, D_2, CH_4; variation intensity from 10^12 to 10^15 molecules per cm^2; stability of intensity about several percent.

b) Monitoring of the all parameters of the equipment should be provided by the computer.

<u>Tentative plan of realization</u>

1.) Design

April 2020

2.) construction:

October 2020

3.) production

December 2020

4.) test at WWUM

May 2021

5.) test at JINR

December 2021

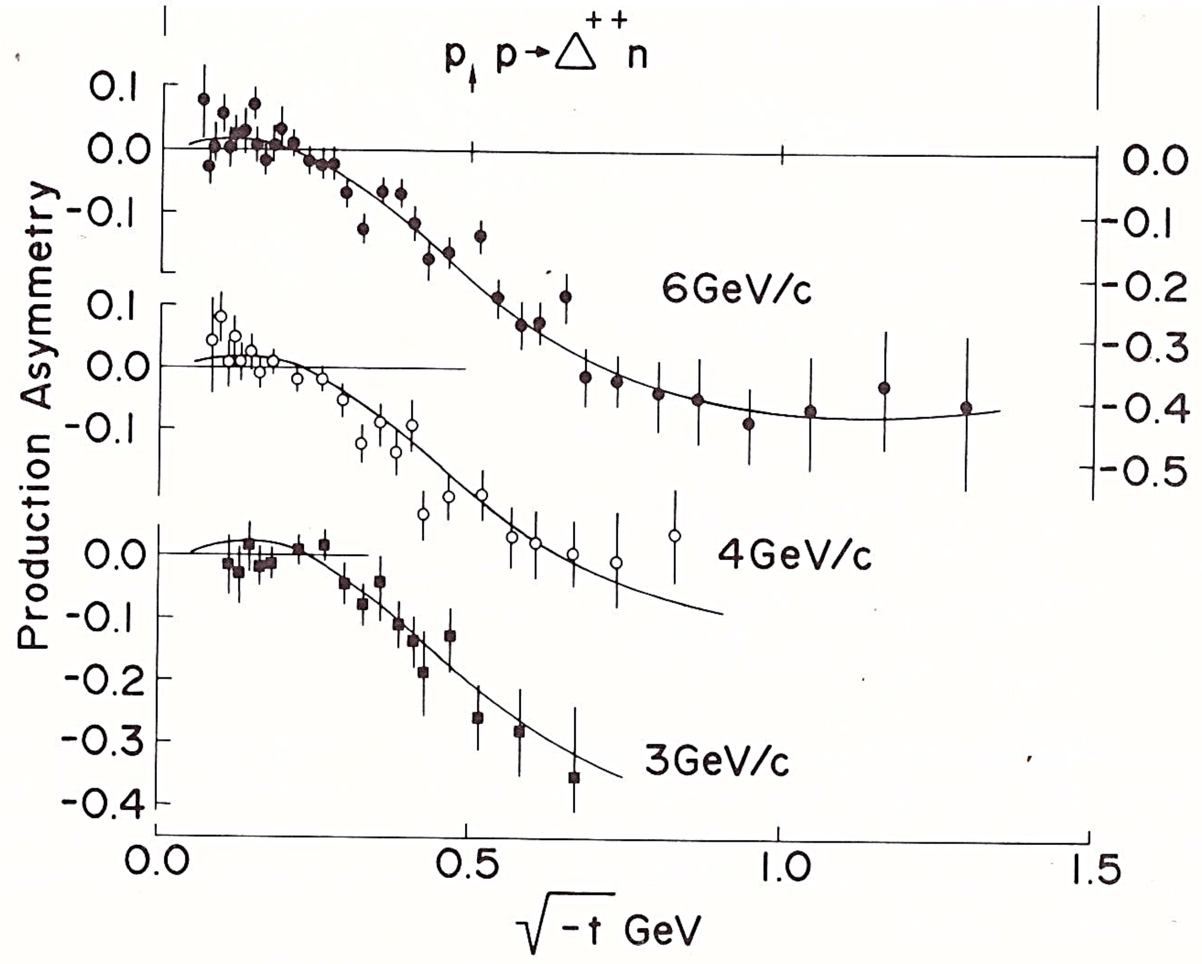

Fig. 1 Overall left-right asymmetries in $p_\uparrow p \to \Delta^{++} n$ at 3, 4, and 6 GeV/c. The curve is an eyeball interpolation of the 6 GeV/c data.

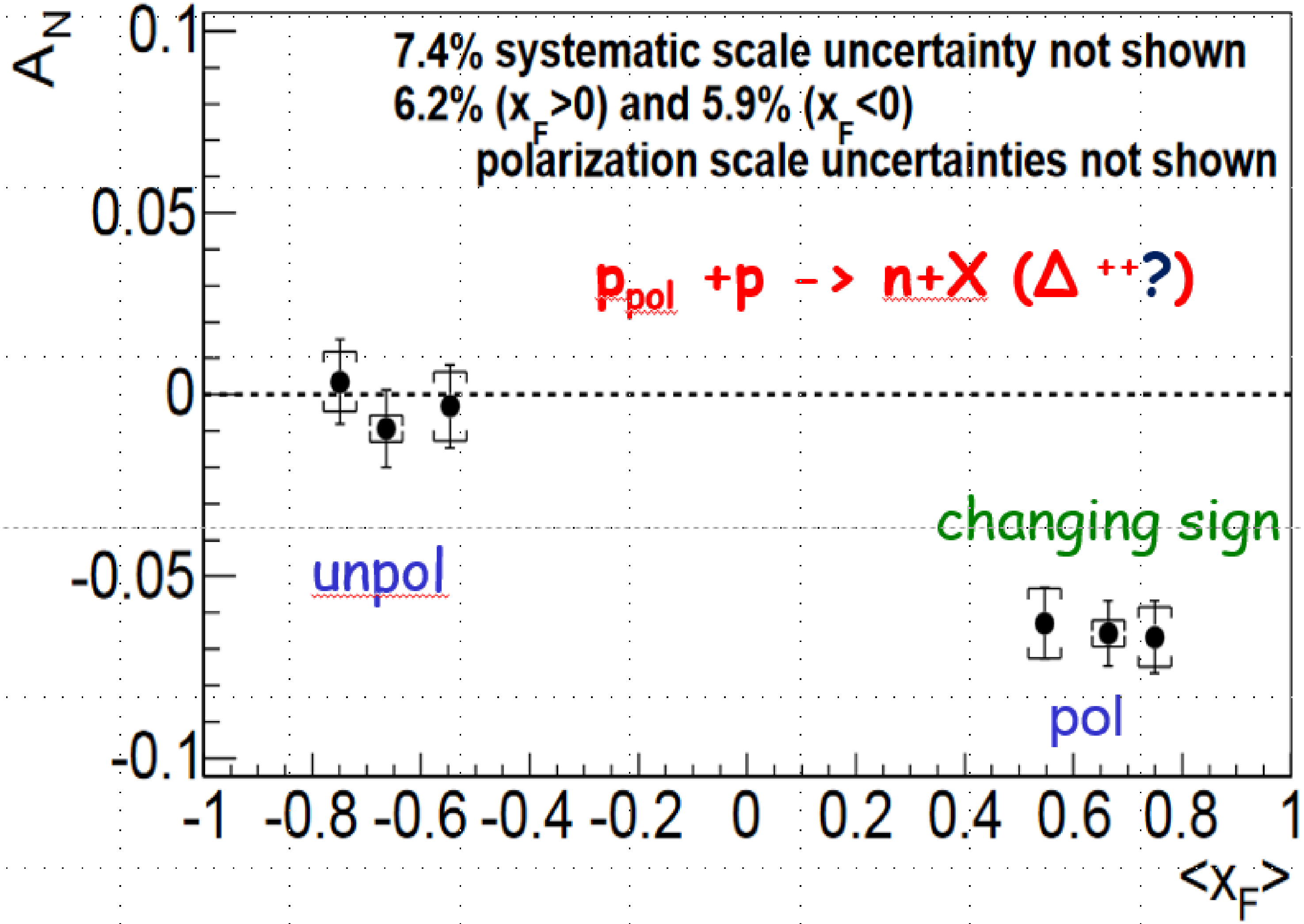

The xF dependence of AN for neutron production in the ZDC⊗BBC trigger sample. The error bars show statistical uncertainties and brackets show pT-correlated systematic uncertainties.